

## A Three-Phase Fluidized Bed Anaerobic Biofilm Reactor Model for Treating Complex Substrates

Mauren Fuentes<sup>a</sup>, Miguel C. Mussati<sup>a</sup>, Pío A. Aguirre<sup>ab\*</sup> and Nicolás J. Scenna<sup>ac</sup>

<sup>a</sup>INGAR -Instituto de Desarrollo y Diseño  
Avellaneda 3657, (3000) Santa Fe, Argentina

<sup>b</sup>Facultad de Ingeniería Química - UNL  
Santiago del Estero 2829, (3000) Santa Fe, Argentina

<sup>c</sup>Departamento de Ing. Qca. -GIAIQ- UTN FRR  
Zeballos 1341, (2000) Rosario, Argentina

### Abstract

The main purpose of this paper is to present a model of a three-phase solid-liquid-gas system to investigate the hydrodynamic and biological behavior and performance of fluidized bed anaerobic biofilm reactors (FBABRs). A general one-dimensional axial dispersive dynamic model is proposed for computing the variation of the properties such as hold-ups and superficial velocities of all phases, biofilm thickness and biological and chemical specie concentrations. Biochemical transformations are assumed occurring only in the fluidized bed zone but not in the free-support material zone. The biofilm process model is coupled to the hydrodynamic model of the system through the biofilm detachment rate, which is assumed as a first-order function of the energy dissipation parameter. Non-active biomass is considered as particulate material subject to hydrolysis. A scheme of carbohydrate degradation, kinetic parameters accepted in the literature and design characteristics of a hypothetical FBABR are taken into account to show the model predictions. The performance of the FBABR is analyzed for different flow patterns through different dispersion coefficients for the phases.

**Keywords:** Anaerobic Processes, Biofilms, Dynamic Simulation, Fluidized Bed Bioreactors, Wastewater Treatment.

### 1. Introduction

Fluidized bed biofilm reactors have received increasing attention as an effective technology for wastewater treatment. A higher biomass concentration than suspended, a smaller pressure drop than fixed bed biofilm systems, no bed-clogging problems, small reactor volumes and low external mass transport resistance are some advantages of the fluidized bed biofilm systems when compared to other biological processes (Yu and Rittmann, 1997). The successful design and operation of a three-phase fluidized bed reactor depend on the ability to accurately predict the main system properties, specifically, the hydrodynamics, the mixing of individual phases and the transfer properties (Muroyama and Fan, 1985). Fluidization characteristics such as fluidized bed height and phase holdups (volume fractions) are critical because of their influence on

---

\* Author to whom correspondence should be addressed: paguir@ceride.gov.ar

the residence time, specific biofilm superficial area in the biologically active zone, reactor size, mass transfer and biofilm detachment rate.

One main difficulty in modeling fluidized bed biofilm reactors is to compute hydrodynamic phenomena (such as bed expansion) and their interaction with the biological variables. Diez Blanco et al. (1995), Bonnet et al. (1997), Yu and Rittmann (1997), Huang et al. (2000), Abdul-Aziz and Asolekar (2000) have studied some aspects of the fluidized bed biofilm reactor hydrodynamics considering steady state fluidization characteristics and hypothetical steady state values for the biofilm thickness. A key feature of the model here proposed is solving simultaneously the dynamic mass balance of the process components and dynamic momentum balance equations in order to describe the hydrodynamics of each phase and the interactions among them in both the hydrodynamic and biological transients.

## 2. Dynamic One-dimensional Model of a Biological Fluidized Bed Reactor

The anaerobic fluidized bed bioreactor is modeled as a three-phase gas-solid-liquid system. The solid phase consists of the inert support particles and the (active and non-active) attached biomass (biofilm). The liquid phase is composed by the chemical species in solution (substrates, intermediates, products, enzymes, ions and water) and (active and non-active) suspended biomass. The gas phase is formed by the gaseous products from degradation stages.

A general axial dispersive model is used to represent the phase behavior. The relationship among the phase volume fractions (holdups)  $\varepsilon_k$  has to verify:

$$\sum_k \varepsilon_k = 1 \quad (1)$$

where  $k$  indicates the liquid ( $k=L$ ), solid ( $k=S$ ) and gas ( $k=G$ ) phases.

The phase mass and momentum balances can be expressed, respectively, as:

$$\partial \frac{\varepsilon_k \rho_k}{\partial t} = -\partial \frac{\varepsilon_k \rho_k U_k}{\partial z} + D_k \partial^2 \frac{\varepsilon_k \rho_k}{\partial z^2} + \sum R_k^{Het} \quad (2)$$

$$\partial \frac{\varepsilon_k \rho_k U_k}{\partial t} = -\partial \frac{\varepsilon_k \rho_k U_k^2}{\partial z} + D_k \partial^2 \frac{\varepsilon_k \rho_k U_k}{\partial z^2} + F_{gk} + F_{pk} + F_{lk} \quad (3)$$

where  $F_{gk}$ ,  $F_{pk}$  and  $F_{lk}$  represent the contribution of the gravity, pressure and interaction forces, respectively (Chen et al., 1999; Hatta et al., 1998);  $U_k$  and  $\rho_k$  represent the superficial velocity and the intrinsic density of each phase, respectively.  $\sum R_k^{Het}$  is the sum of all heterogeneous reactions for phase  $k$ .

For a specie concentration  $\phi_k$ , the mass balance is expressed as:

$$\partial \frac{\varepsilon_k \phi_k}{\partial t} = -\partial \frac{\varepsilon_k \phi_k U_k}{\partial z} + D_k \partial^2 \frac{\varepsilon_k \phi_k}{\partial z^2} + \sum R_{\phi_k} \quad (4)$$

where  $\sum R_{\phi_k}$  is the sum of all homogeneous and heterogeneous reactions where  $\phi_k$  is involved.

In addition to mass balance equations for biological and chemical species, the model includes the system charge balance (electroneutrality condition) for calculating pH and the bioparticle model. Algebraic and differential balance equations are not here included due to space restrictions.

## 2.1 Bioparticle model and fluidization characteristics

Homogeneous biofilm distribution on the support particles, constant density and diameter of the support particles, constant wet biofilm density and spherical geometry are assumed for the bioparticle model (Abdul-Aziz and Asolekar, 2000).

The solid holdup  $\varepsilon_s$  varies during the biological time horizon (BTH) due to the ongoing microbiological processes: growth, death, detachment and hydrolysis of biomass. Gas holdup also varies but its contribution is generally negligible compared to the solid and liquid holdups in anaerobic reactors. Even when these microbiological processes cause a time variation of the bed porosity, this change is sufficiently slow compared to those caused by a hydrodynamic transient. A biofilm thickness increase causes an increase in the total height  $H$  of the fluidized bed, which is calculated as follows:

$$H = \frac{W}{\rho_p A_C \left[ \frac{1}{H} \int_z \varepsilon_s dz \right]} \left[ \frac{1}{H} \int_z \left( 1 + \frac{2\delta}{d_p} \right)^3 dz \right] \quad (5)$$

where  $W$ ,  $\rho_p$ ,  $d_p$ ,  $A_C$  and  $\delta$  are the initial particle load, particle density and diameter, column cross section area and biofilm thickness, respectively.

The liquid and gas phase densities can be assumed time- and space-invariant in BTH and in the hydrodynamic time horizon (HTH). The solid density is a function of the biofilm thickness, which can be considered invariant in HTH but not in BTH.

## 2.2 Initial and Boundary Conditions

Perfect mixture hypothesis is considered as initial condition. For hydrodynamic variables a static bed condition is assumed. Since the biofilm adsorption phenomenon is not modeled, low steady state concentration values are assigned as initial condition values for the biological and chemical species.

Danckwerts-type boundary conditions are considered at the reactor inlet ( $z=0$ ) for the species referred to the liquid phase. The boundary conditions for the species referred to the solid and gas phases are given by the no-flux condition at the reactor inlet. A general zero derivative boundary condition is considered at the reactor outlet ( $z=H$ ).

## 3. Computational Aspects

The mathematical model was implemented and solved using the process modeling software tool gPROMS (Process Systems Enterprise Ltd). An axial dimensionless model was derived since gPROMS does not permit to calculate moving boundary problems in direct form. The axial dimensionless length is defined as follows:

$$z^* = \frac{z}{H}, 0 \leq z^* \leq 1, dz = H dz^* \quad (6)$$

Backward (BFDM) and centered (CFDM) finite difference methods were used to solve the PDEs. Using BFDM and CFDM of second order over a uniform grid of 20 intervals the total CPU time is about 100 seconds on a 800 MHz Pentium IV PC.

## 4. Performance analysis of a FBABR in both BTH and HTH

### 4.1 Anaerobic degradation scheme

In order to show model capabilities and results, a simplified anaerobic digestion model involving a mesophilic consortium is chosen since hydrodynamics is independent of the

degradation stage number. The scheme assumes carbohydrates as characteristic compounds of organic contamination. Insoluble carbohydrates are enzymatically hydrolyzed to soluble carbohydrates, which are assumed as glucose (Angelidaki et al., 1999). The glucose degradation process involves four microorganism (m.o.) groups: 1) acidogens, which use glucose to produce a mixture of acetic, propionic and butyric acids; 2) propionic and 3) butyric acetogens, which convert respectively propionic and butyric acids into acetic acid; and finally, 4) methanogens. As the specific growth rate of the utilizing-hydrogen methanogenic m.o. is much faster than acetoclastic methanogens (degradation of acetic acid into methane and carbon dioxide), the utilizing-hydrogen methanogenic stage is combined with acetogenic stages (Angelidaki et al., 1993, 1999). Thus, the acetoclastic methanogens are only included in the model. The three components considered in the gas phase are methane, carbon dioxide and water vapor. As the ammonia levels at the pH ranges of anaerobic reactors in operation are quite low, ammonia in the gas phase is not considered.

#### 4.2 Model Parameters and Constants

The anaerobic digestion process stoichiometry for glucose degradation given in Angelidaki et al. (1993) is used. The specific growth and death rates of m.o. are assumed to be the same for suspended and attached biomass. Non-active biomass is considered as particulate material subject to hydrolysis, and the specific biomass hydrolysis rate is the same for all species (Angelidaki et al., 1999). The biofilm process model is coupled to the system hydrodynamic model through the biofilm detachment rate, which is assumed as a first-order function on the energy dissipation parameter (Huang and Wu, 1996) and on the mass fraction of each specie in the biofilm, and a second-order function on the biofilm thickness. The specific detachment rate is assumed the same for all biological species.

#### 4.3 Study Case

A 10 g COD L<sup>-1</sup> concentration of a synthetic substrate (70% glucose, 20% acetate and 10% milk powder) is fed at a flow rate of 3.5 L d<sup>-1</sup>. The bioreactor consists of a 200 cm high column with 8 cm diameter. The static bed height is 80 cm for a load of 4250 g of support material. The mean diameter and density of support particles are 0.03 cm and 2630 g cm<sup>-3</sup>, respectively.

#### 4.4 Simulation Results and Analysis

Model predictions considering the two ideal flow patterns for the phases i.e. plug flow ( $D_k=0$ ) and perfect mixture ( $D_k=\infty$ ) and non-ideal flow ( $D_k>0$ ) were analyzed. Following, some results assuming  $D_G=\infty$  and a constant and comparatively small gas holdup with respect to the other phases are commented. With these assumptions, the bioreactor behaves as a two-phase (solid-liquid) pseudo-system from a hydrodynamic point of view since the formation of the gas phase as a consequence of fermentation products has a little effect over the hydrodynamic behavior. However, the mass and momentum balances are rigorously solved for the three phases involved. The liquid phase dispersion coefficient is  $D_L=9.16$  cm<sup>2</sup> s<sup>-1</sup> calculated as in Kim and Kim (1983). The solid phase dispersion coefficient was varied from  $D_S=0$  to  $D_S=5.8$  cm<sup>2</sup> s<sup>-1</sup>. The latter guarantees homogeneous profiles of species in the solid phase. The time predicted to reach the hydrodynamic steady state condition from the static bed condition is approximately 0.001 to 0.002 days depending on the phase dispersion coefficient values for a reactor inlet velocity of 0.45 cm s<sup>-1</sup> (Fig. 1). Bed expansions around 46% are reached during HTH. Changes in the porosity of fluidized bed bioreactors due to biofilm development or biofilm detachment are less significant compared to changes in

the height of the bed. Fig. 2 shows variations of approximately 0.32% and 5.2% in bed porosity and height, respectively, for the dispersive model during BTH. Very similar results were obtained for the convective model.

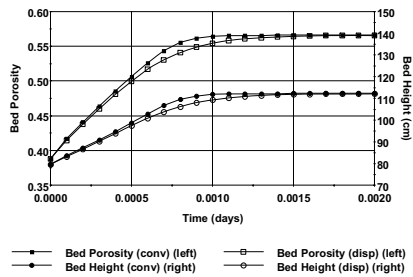


Fig. 1. Bed porosity and height in HTH

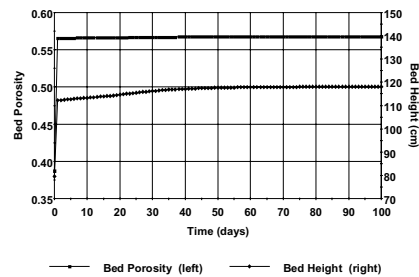


Fig. 2. Bed porosity and height in BTH

Total biofilm concentration is almost uniform along the axial direction of the bed for a dispersive model in the liquid and solid phases but a significant decrement of biofilm concentration is predicted instead using a plug flow model (Fig. 3 and 4).

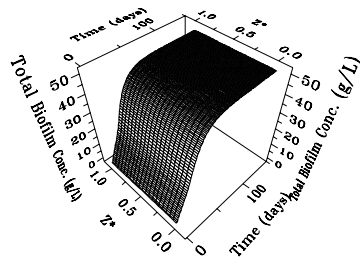


Fig. 3. Total biofilm concentration profile (dispersive model)

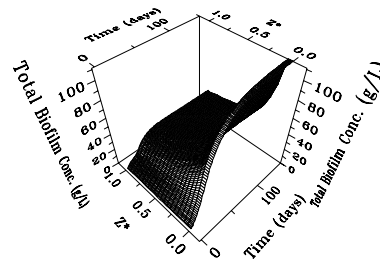


Fig. 4. Total biofilm concentration profile (convective model)

The relationship between biofilm thickness and attached biomass concentration is hardly dependent on the bioparticle model, e.g. a 3  $\mu\text{m}$  steady state biofilm thickness is reached using a dispersive model. In this case a spherical geometry and homogeneous biofilm distribution on the inert support particles are assumed. The biofilm is normally inhomogeneously distributed on the real support particles. It depends on particle characteristics (shape, roughness, material porosity, size and weight) and on the hydrodynamic conditions, such as the fluid erosion on the bioparticle surface. This means that if a more realistic bioparticle model is included into the general model, a more precise relation between the total (active and non-active) attached biomass concentration and biofilm thickness values is predicted.

The steady state substrate concentration is approximately reached after 25 days. The soluble and total COD and pH values at the bed outlet ( $z^*=1$ ), for the dispersive model, are shown in Fig. 5. Even though substrate concentration remains almost constant, the m.o. concentration in liquid and solid phases varies due to the soluble substrate fraction (glucose) produced during the hydrolysis of non-active biomass. A biological steady state condition is reached at day 80 (Fig. 3 and 4). The biological steady state is sensitive to the specific biofilm detachment rate. An increase of 20% in this parameter predicts a decrease of 8.6% and 12.5% in the total biofilm concentration and time required to reach the biological steady state, respectively.

Independently of the phase dispersion coefficient values, the largest changes on the hydrodynamic properties evidently occur during HTH. The liquid phase velocity varies during HTH and reaches the hydrodynamic steady state as shown in Fig. 6. This property suffers a little decrease due to the biofilm increase for all model variations during BTH.

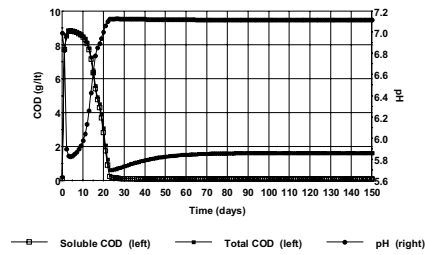


Fig. 5. COD and pH in BTH

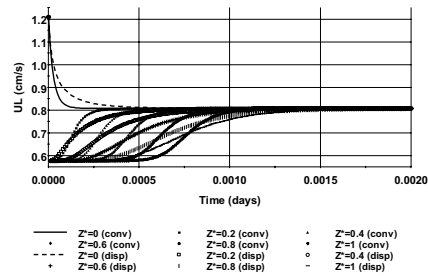


Fig. 6. Liquid phase superficial velocity in HTH

The solid superficial velocity is practically zero compared to the liquid one when the fluidized bed reaches the hydrodynamic steady state (Fig. 7). However, a variation is observed in BTH while biofilm concentration reaches the biological steady state values (Fig. 8).

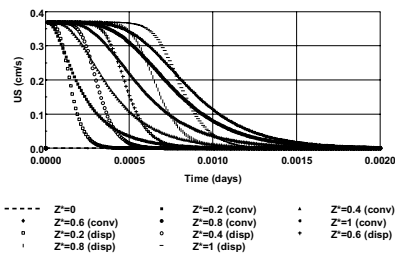


Fig. 7. Solid phase superficial velocity in HTH

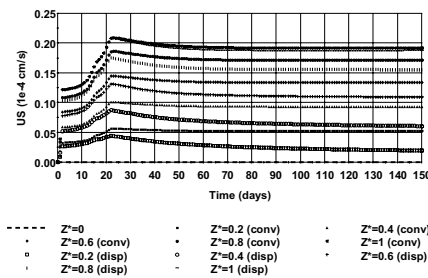


Fig. 8. Solid phase superficial velocity in BTH

## References

- Abdul-Aziz, M.A. and S. R. Asokelar, 2000, *Wat. Env. Res.* 72, 105.  
 Angelidaki, I., L. Ellegaard and B.K Ahring, 1999, *Biotechnol. Bioeng.* 63 (5), 363.  
 Angelidaki, I., L. Ellegaard and B.K. Ahring, 1993, *Biotechnol. Bioeng.* 42, 159.  
 Bonnet, B., D. Dochain and J.P Steyer, 1997, *Wat. Sci. Technol.* 36 (5), 285.  
 Chen, Z., L.G. Gilibaro and P.U. Foscolo, 1999, *Ind. Eng. Chem. Res.* 38, 610.  
 Diez Blanco, V., P.A. García Encina and F. Fdz-Polanco, 1995, *Wat. Res. (G.B.)* 29 (7), 1649.  
 Hatta, N., H. Fujimoto, M. Isobe and J.S. Kang, 1998, *J. Multiphase Flow*, 24 (4), 539.  
 Huang, J. and C. Wu, 1996, *Biotechnol. Bioeng.* 50, 643.  
 Huang, J., J. Yan and C. Wu, 2000, *J. Chem. Technol. Biotechnol.* 75, 269.  
 Kim, S.D. and C.H. Kim, 1983, *J. Chem. Eng. Japan*, 16, 172.  
 Muroyama, K., L.S Fan, 1985, *AICHE J.* 31, 1.  
 Yu, H. and B.E. Rittmann, 1997, *Wat. Res.* 31 (10), 2604.

## Acknowledgements

The financial support from CONICET, ANPCyT and UNL is acknowledged.